Structural and Electronic Properties of Cadmium Sulfide Clusters

Jan-Ole Joswig,[†,§] Michael Springborg,*[,†] and Gotthard Seifert[‡,||]

Fakultät für Chemie, Universität Konstanz, D-78457 Konstanz, Germany, and Fachbereich 6—Physik, Universität-GH Paderborn, D-33098 Paderborn, Germany

Received: September 30, 1999; In Final Form: December 9, 1999

Crystalline cadmium sulfide is a semiconductor for which the wurtzite and zinc blende structures are energetically almost degenerate. Due to quantum-confinement effects, it is possible to tune the optical properties of finite cadmium sulfide clusters by varying their size. Here, we report results of a theoretical study devoted to the properties of stoichiometric Cd_nS_n clusters as a function of their size n. We have optimized the structure, whereby our initial structures are spherical parts of either of the two crystal structures, and we have studied systems with up to almost 200 atoms. The calculations were performed by using a simplified LCAO-DFT-LDA scheme. The results include the structure, electronic energy levels (in particular the frontier orbitals HOMO and LUMO), and stability as a function of size. The results allow for a unique definition of a surface region. The Mulliken populations indicate that the bonds within this region are more ionic than in the bulk. Furthermore, whereas the HOMO is delocalized over major parts of the nanoparticle, the LUMO is a surface state, which confirms recent experimental findings. Finally, the relative stability of the zinc blende and wurtzite structures is strongly dependent on the size of the system, and there is a close connection between the HOMO-LUMO energy gap and stability.

1. Introduction

During the past two decades experimental and theoretical studies of semiconductor nanoparticles have become increasingly important. One of the main reasons for studying these systems is that their electronic properties can be tuned through varying their size. In the simplest approximation, this quantum-size effect (QSE) or quantum-confinement effect[1−5] can be considered as an experimental realization of the *particle in a box*.

Such particles can be produced in solution, and through proper choice of catalysts it has become possible to produce systems with increasingly well-defined size. In some cases, the dangling bonds on their surfaces are saturated by surfactants. Alternatively, semiconductor nanoparticles are produced as quantum dots and then embedded in another semiconductor host.

As a prototypical example we shall here consider cadmium sulfide clusters. Similar to many other $A^{II}B^{VI}$ semiconductors it can, under standard conditions, crystallize in one of two possible lattice structures, i.e., the zinc blende and the wurtzite structure. For crystalline cadmium sulfide, however, these two forms are energetically almost degenerate with the wurtzite structure being slightly more stable.[6,7]

Due to the interest in the variation of the electronic properties as a function of system size, there has been a number of theoretical studies devoted to the properties of Cd_nS_m clusters, whereby both stoichiometric ($n = m$) and nonstoichiometric ($n \neq m$) clusters have been considered. Independent of $n = m$ or $n \neq m$, such studies are complicated since the experimentally interesting systems have $n + m$ in the range 100−10000 which is large for more accurate electronic-structure methods. On the other hand, the systems possess a relatively low symmetry (i.e., the atoms near the surfaces have different surroundings than those in the inner parts). Therefore, electronic-structure calculations have to employ various approximations in order to become possible.

In some of the studies on cadmium sulfide clusters or the chemically related systems cadmium selenide and cadmium telluride the effective-mass method has been applied in order to study the energetically lowest optical transitions.[8−12] Thereby, the underlying structure of the cluster becomes of only secondary importance. Alternatively, tight-binding methods have been applied on these systems,[13−27] and it has almost exclusively been assumed that the structure of the cluster is as that of a finite part of the infinite crystal. It should, however, be obvious that the properties may depend sensitively on possible structural relaxations and, for CdS, that the near-degeneracy of the zinc blende and wurtzite crystalline structures may lead to extra effects when studying the properties as functions of system size. Nevertheless, almost all previous theoretical studies have not taken structural relaxations into account, except for recent studies of Whaley and co-workers,[13,26,27] who used an sp^3s^* tight-binding model, and the density-functional work of Eichkorn and Ahlrichs,[22] who studied smaller CdSe clusters with surfactants. Only in one of their studies, Whaley and co-workers optimized the structure.[26] Finally, to our knowledge, all theoretical studies have considered clusters derived from either the wurtzite or the zinc blende crystal structure and there has so far been no theoretical comparison of the two types of clusters.

In the present work we shall explicitly study how the electronic and structural properties of stoichiometric Cd_nS_n clusters depend on n for n up to approximately 100. We have considered spherical parts of both wurtzite and zinc blende crystals and, subsequently, let their structures relax to their closest total-energy minimum whereby all atoms were allowed to move. The center of the initial spherical parts was chosen as

* Corresponding author. E-mail: mcs@chclu.chemie.uni-konstanz.de.
† Universität Konstanz.
‡ Universität-GH Paderborn.
§ E-mail: jj1@chclu.chemie.uni-konstanz.de.
|| E-mail: seifert@phys.uni-paderborn.de.

10.1021/jp993512c CCC: $19.00
Published on Web 03/07/2000

the midpoint of a Cd−S nearest-neighbor bond, which ensures that all clusters become stoichiometric. We shall explicitly discuss the structural relaxations and how these influence the electronic properties as well as compare the zinc blende- and the wurtzite-derived clusters.

The article is organized as follows: in section 2, a brief overview of the density-functional method is given and results of test calculations for systems with periodic boundary conditions are presented; in section 3, the results of the calculations on various finite clusters are presented and discussed; and, in section 4, our conclusions are summarized.

2. Method of Calculation

The calculational method has been described in detail elsewhere.[28−31] Therefore, we just give a brief overview and refer the reader who is interested in more details to those references.

The approximate LCAO-DFT-LDA method is based on the density-functional theory of Hohenberg and Kohn[32] in the formulation of Kohn and Sham.[33] The single-particle eigenfunctions $\psi_i(\mathbf{r})$ to the Kohn−Sham equations are expanded in a set of atomic-like basis functions φ_m:

$$\psi_i(\mathbf{r}) = \sum_m c_{im}\,\varphi_m(\mathbf{r}) \tag{1}$$

Here, m is a compound index that describes the atom at which the function is centered, the angular dependence of the function, as well as its radial dependence. These functions are obtained from self-consistent density-functional calculations on the isolated atoms employing a large set of Slater-type basis functions.

The Hamiltonian is defined as

$$\hat{h} = \hat{t} + V_{\text{eff}}(\mathbf{r}) \tag{2}$$

Here, $\hat{t}$ is the kinetic-energy operator, and the effective Kohn−Sham potential $V_{\text{eff}}(\mathbf{r})$ is approximated as a simple superposition of the potentials of the neutral atoms:

$$V_{\text{eff}}(\mathbf{r}) = \sum_j V_j^0(|\mathbf{r} - \mathbf{R}_j|) \tag{3}$$

Furthermore, we make use of a tight-binding approximation, so that

$$h_{mn} = \langle\varphi_m|\hat{t} + \sum_j V_j^0|\varphi_n\rangle = \langle\varphi_m|\hat{t} + V_{jm}^0 + (1 - \delta_{jn,jm})V_{jn}^0|\varphi_n\rangle \tag{4}$$

where $\mathbf{R}_{jm}$ and $\mathbf{R}_{jn}$ are the positions of the atoms at which the mth and nth basis functions are centered, respectively. The Kronecker-δ is included in order to assure that the potential is not double-counted for $j_n = j_m$. Through this approximation, only two-center terms in the Hamiltonian matrix are considered, but all two-center terms ($h_{mn} = \langle\varphi_m|\hat{h}|\varphi_n\rangle$, $S_{mn} = \langle\varphi_m|\varphi_n\rangle$) are calculated exactly within the Kohn−Sham basis.

The approximations lead to the same structure of the secular equations,

$$\sum_m c_{im}(h_{mn} - \epsilon_i S_{mn}) = 0 \tag{5}$$

as in (nonorthogonal) tight-binding (TB) schemes, but it is important to stress that all matrix elements are calculated and none is determined through fitting to experimental results. Furthermore, in contrast to the method of Leung and Whaley[26] the present method does not rely on any assumption on whether atoms are considered bonded.

Using the Kohn−Sham eigenvalues ϵ_i, the total energy $E[\rho(\mathbf{r})]$ may be written as

$$E[\rho(\mathbf{r})] = \sum_i^{\text{occ}}\epsilon_i - \frac{1}{2}[\int V_{\text{eff}}(\mathbf{r})\rho(\mathbf{r})\mathrm{d}\mathbf{r} - \int V_{\text{ext}}(\mathbf{r})\rho(\mathbf{r})\mathrm{d}\mathbf{r}] + E_{\text{XC}} - \frac{1}{2}\int V_{\text{XC}}(\mathbf{r})\rho(\mathbf{r})\mathrm{d}\mathbf{r} + E_{\text{N}} \tag{6}$$

The external potential V_{ext} is the electrostatic potential from the nuclei, E_{XC} is the exchange-correlation energy, V_{XC} the corresponding potential, and E_{N} the nuclear repulsion energy.

Since the difference between superposed atomic electron densities and the true electron density of the system of interest is only small, and since by far the largest parts of the interatomic interactions are of fairly short range, the major part of the binding energy is contained in the difference of the single-particle energies of the system of interest, $\{\epsilon_i\}$, and of the isolated atoms, $\{\epsilon_{jm}\}$ (ϵ_{jm} is the jth eigenvalue of the mth atom), i.e.,

$$\epsilon_{\text{B}} \equiv \sum_i^{\text{occ}}\epsilon_i - \sum_j\sum_m\epsilon_{jm} \tag{7}$$

The short-ranged interactions can be approximated by simple pair-potentials, so that we end up with the following expression for the binding energy:

$$E_{\text{B}} \approx \sum_i^{\text{occ}}\epsilon_i - \sum_j\sum_m\epsilon_{jm} + \frac{1}{2}\sum_{j\neq j'}U_{jj'}(|\mathbf{R}_j - \mathbf{R}_{j'}|) \tag{8}$$

$U_{jj'}(|\mathbf{R}_j - \mathbf{R}_{j'}|)$ is determined as the difference of ϵ_{B} and $E_{\text{B}}^{\text{SCF}}$ for diatomic molecules (with $E_{\text{B}}^{\text{SCF}}$ being the total energy from exact density-functional calculations), i.e., in our study for CdS, Cd_2, and S_2 molecules. Subsequently, it is written as a short-ranged polynomial

$$U(R) = \begin{cases} P_n(R - R_1) & \text{for } R < R_1, \\ 0 & \text{for } R \geq R_1, \end{cases} \tag{9}$$

with P_n being the polynomial whose order typically is $n = 4$. Different pair potentials have different polynomials P_n and cutoff radii R_1.

Finally, all electrons except for the 4d and 3d electrons of Cd and the 3s and 3p electrons of S were treated within a frozen-core approximation.

By fitting to results of parameter-free density-functional calculations on diatomics that in turn are known to provide an accurate description of structural properties and of relative total energies of different isomers also our computational method possesses these characteristics. On the other hand, just as the density-functional calculations, we do not expect the method to yield accurate dissociation energies. Furthermore, since our method employs a minimal basis set and since the density-functional formalism mainly is a ground-state formalism, we have not attempted to calculate excitonic excitation energies.

As is obvious from the discussion above, the present calculational scheme is constructed as being accurate for small (diatomic) molecules, whereas we attempt to use it for larger clusters. Therefore, to obtain an estimate of the accuracy of the method, we first performed calculations on the two crystalline

TABLE 1: Results of the Calculations with Periodic Boundary Conditions: Lattice Parameters and Bond Lengths in Zincblende and Wurtzite Crystals and Energy Difference in Comparison with Results of Other Theoretical and Experimental Studies

structure	parameter	this work	exp. [34]	theory [6, 35]
zincblende	*a*	5.7897 Å	5.818 Å	5.811 Å
	bond length	2.5070 Å	2.5193 Å	2.5162 Å
wurtzite	*a*	4.0985 Å	4.1248 Å	4.121 Å
	c	6.6891 Å	6.749 Å	6.682 Å
	bond length	2.5097 Å	2.5265 Å	2.5216 Å
	ΔE_{W-Z}/atom[a]	+3.5 meV		−1.1 meV

[a] ΔE_{W-Z} is positive (negative) when the zincblende (wurtzite) structure is stabler.

structures, zinc blende and wurtzite. The calculated lattice constants and the difference in the total energies of the two structures are then, when compared with other theoretical or experimental information, estimates of this accuracy.

Since these calculations assume a periodically repeated unit cell (i.e., the calculations were performed for $\boldsymbol{k} = \mathbf{0}$), it was necessary first to determine how large this should be so that finite-size effects were negligible, and, simultaneously, that the two structures could be described with unit cells of the same size. It turned out that this was the case for unit cells of 72 pairs of atoms. Moreover, the unit cells of the two structures have then nearly the same volume.

Subsequently, we optimized the structure by varying the lattice constants. In Table 1 our results are compared with experimental[34] and theoretical data.[6,35] One observes a good agreement between all theoretical works and the experimental results. In particular, the bond lengths differ by less than 1%, and our calculations reproduce the energetical near-degeneracy of the two crystal structures within 5 meV/atom, which we then consider the accuracy of the calculations (notice that for the crystals we have no surface effects as for the clusters and that the calculations have been parametrized for diatomic molecules for which the atoms have a very different coordination). Our crystal calculations suffer, however, from predicting that the zinc blende structure is the stabler crystal structure. Experimental studies[34] have indicated that the wurtzite structure is stabler than the zinc blende structure, but, to our knowledge, there exists no experimental information on their relative total energies.

3. Results

We now turn to our main results, i.e., those for finite Cd_nS_n clusters. In describing the structural properties of those we shall discuss only the radial distribution of atoms as described below. On the other hand, we shall discuss different electronic properties as functions of cluster size, i.e., the Mulliken gross populations, the densities of states (DOS), the spherical average of the atomic contributions to single molecular orbitals, especially those of the highest occupied and lowest unoccupied molecular orbitals (HOMO and LUMO). We will also analyze the size dependence of the HOMO and LUMO energies as well as of the total energy per CdS pair. All quantities will be considered as functions of cluster size as well as of whether the clusters were constructed as finite parts of the zinc blende or the wurtzite crystal structure.

The radial distribution is defined as follows. For each atom of the Cd_nS_n cluster we calculate the distance to the center of the cluster,

$$\mathbf{R}_0 = \frac{1}{2n}\sum_{j=1}^{2n}\mathbf{R}_j \qquad (10)$$

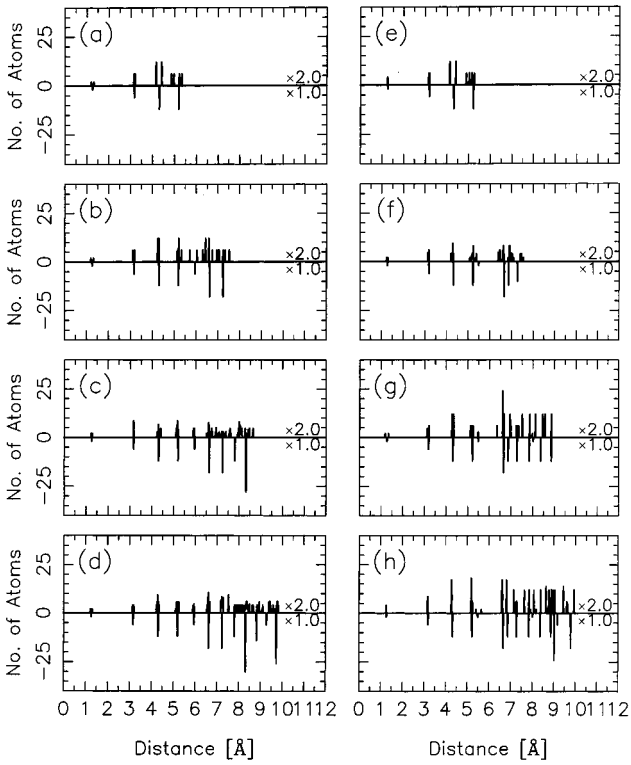

Figure 1. Radial distribution of cadmium and sulfur atoms for zinc blende (left column) and wurtzite (right column) clusters of different sizes: (a), (e) $Cd_{16}S_{16}$; (b), (f) $Cd_{37}S_{37}$; (c), (g) $Cd_{57}S_{57}$; and (d), (h) $Cd_{81}S_{81}$. The results for the optimized clusters are shown as the upper curves, whereas the lower curves show those for the initial clusters.

Subsequently, all these 2*n* distances are depicted in a single diagram.

Figure 1 shows the radial distributions of eight different clusters with either zinc blende (left column) or wurtzite structure (right column). Each panel shows the distances for both cadmium and sulfur atoms of the optimized structure (upper half part) and of the initial geometry (lower half part). It is clearly recognized that for the optimized structures the largest changes compared with the initial structure occur in the outer parts (i.e., up to 2−3 Å from the outermost atoms). In this region, some atoms move away from the center of the cluster, whereas others approach the center. Inspecting the results in details shows that only sulfur atoms move outward, whereas the cadmium atoms move inward. Similar structural relaxations were also found by Leung and Whaley[26] in their study of wurtzite-derived clusters. Cadmium, being a typical metal atom, prefers a high coordination, whereas sulfur atoms for many systems prefer a low coordination of 2.

In Figure 2 we show the atomic Mulliken gross populations for the different clusters as functions of the distance of the corresponding atom to the center for the same representative clusters as were presented in Figure 1. In this figure it is clearly seen that in the inner parts of the clusters, the gross populations are very close to the values for the neutral atoms, implying that the bonds in this region are mainly covalent. On the other hand, in the outermost region, there is a transfer of electrons from the cadmium atoms to the sulfur atoms in agreement with the larger electronegativity of sulfur. The boarder between those two regions coincides with that mentioned above and lies roughly 2.5 Å from the outermost atoms.

In total all these results suggest that the stoichiometric Cd_nS_n clusters (for which there are both Cd and S atoms at the surface) possess a surface region of about 2.5 Å thickness. Experimental

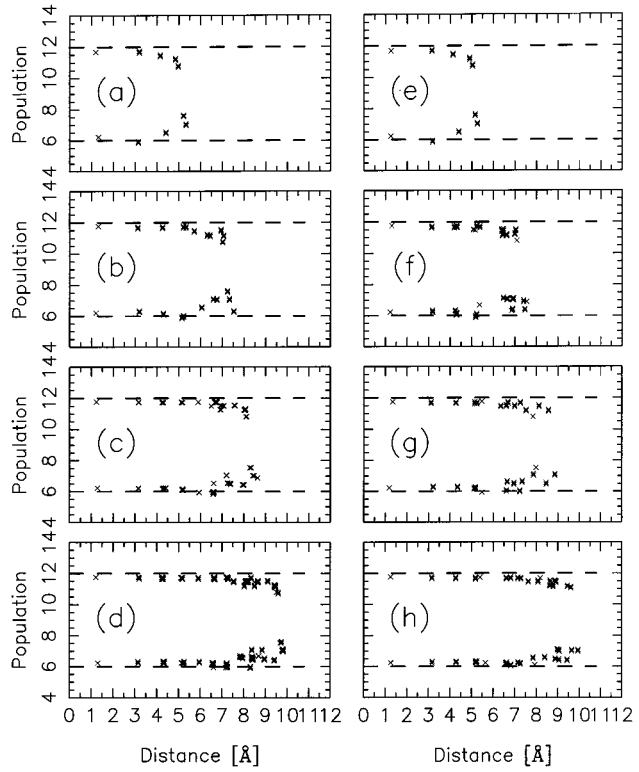

Figure 2. Radial distribution of Mulliken populations for zinc blende (left column) and wurtzite (right column) clusters of different sizes: (a), (e) $Cd_{16}S_{16}$; (b), (f) $Cd_{37}S_{37}$; (c), (g) $Cd_{57}S_{57}$; and (d), (h) $Cd_{81}S_{81}$. The horizontal dashed lines mark the values for the neutral atoms, i.e., 12 for cadmium and 6 for sulfur atoms.

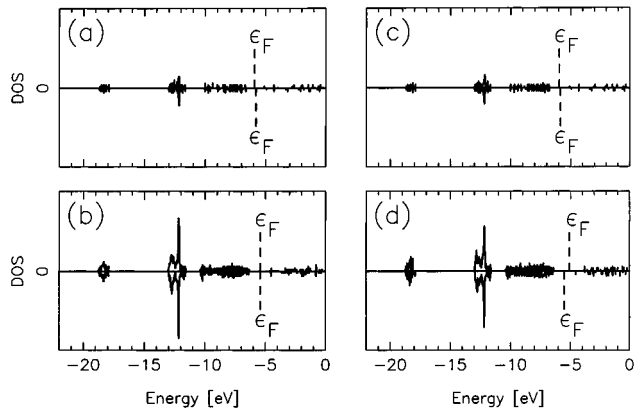

Figure 3. Density of states (DOS) for zinc blende (left column) and wurtzite (right column) clusters of different sizes: (a), (c) $Cd_{16}S_{16}$; and (b), (d) $Cd_{81}S_{81}$. The curves pointing upward are those for the optimized clusters, whereas those pointing downward are for the initial structures. The vertical dashed lines marked ϵ_F show the Fermi energy.

and theoretical studies of surfaces of CdS and CdSe[36−38] have given results that are very similar to ours, i.e., the surface relaxations are found in the outermost two layers of atoms which correspond to a thickness of roughly 2.5 Å, and, moreover, the outermost Cd atoms move inward whereas the S or Se atoms move outward. Finally, in our cluster calculations the structural relaxations were never so large that Cd−Cd or S−S nearest-neighbor bonds were formed, although this may be a consequence of our chosen initial structures (spherical parts of the crystalline structures) for which such bonds were absent, too.

Figure 3 shows the densities of states of four different clusters. It is observed that the states below the Fermi energy tend to arrange into separate bands. There is one such band between

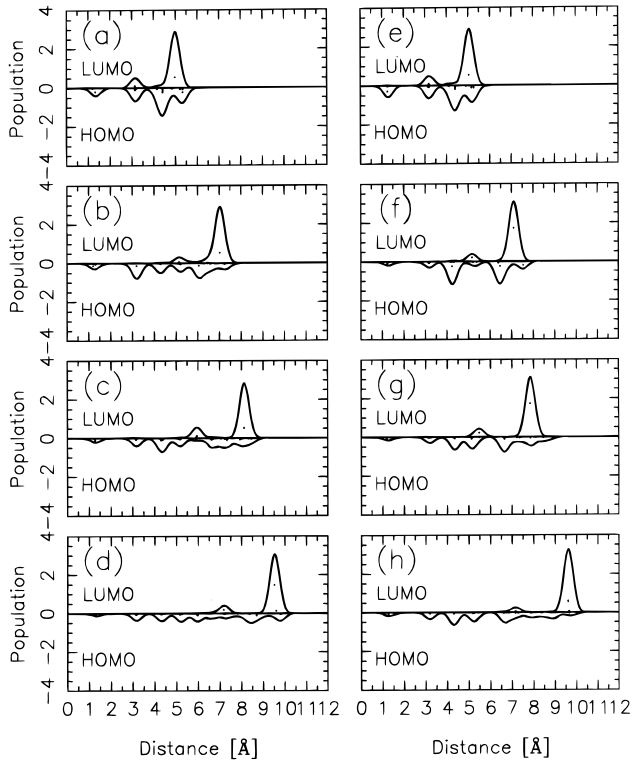

Figure 4. Spherical average of the atomic contributions to HOMO (pointing downward) and LUMO (pointing upward) broadened with Gaussian-type functions for zinc blende (left column) and wurtzite (right column) clusters of different sizes: (a), (e) $Cd_{16}S_{16}$; (b), (f) $Cd_{37}S_{37}$; (c), (g) $Cd_{57}S_{57}$; and (d), (h) $Cd_{81}S_{81}$.

−19 and −18 eV which is mainly due to sulfur 3s functions, another between −13 and −11.5 eV due to cadmium 4d functions, and one between −10.5 and −6.5 eV due to both cadmium 5s and sulfur 3p functions. For both crystal structures, zinc blende and wurtzite, these three bands lie in the same energy regions. For the bigger clusters the bands broaden slightly, but are otherwise largely unchanged. This tendency to form bands with increasing cluster size has already been described by others (see, e.g., refs 39−41), and the overall behavior is in excellent agreement with results on crystalline CdS.[36−38,42−44]

Often, stability is related to the occurrence of an energy gap between occupied and unoccupied orbitals, and for most of the systems we have studied (including some of those of the figure) the relaxations lead to a small increase of these energy gaps.

Figure 4 shows a schematic representation of the spatial dependence of the HOMO and LUMO. This representation has been constructed as follows. With N_{ij} being the Mulliken gross population for the jth atom and ith orbital we define the following density:

$$\tilde{\rho}_i(\mathbf{r}) = \sum_j N_{ij} \left(\frac{2\alpha}{\pi}\right)^{3/2} \exp[-\alpha(\mathbf{r} - \mathbf{R}_j)^2] \qquad (11)$$

with α being a chosen, fixed constant. Subsequently, we calculate the spherical average of this density, which is the one depicted in the figure.

The most important observation in Figure 4 is an increasing delocalization of the HOMO to the complete cluster and a simultaneous localization of the LUMO to the surface atoms with increasing cluster size. In all cases the LUMO is localized to between one and three surface atoms. Therefore, in contrast to the HOMO, the energy of the LUMO depends very sensitively

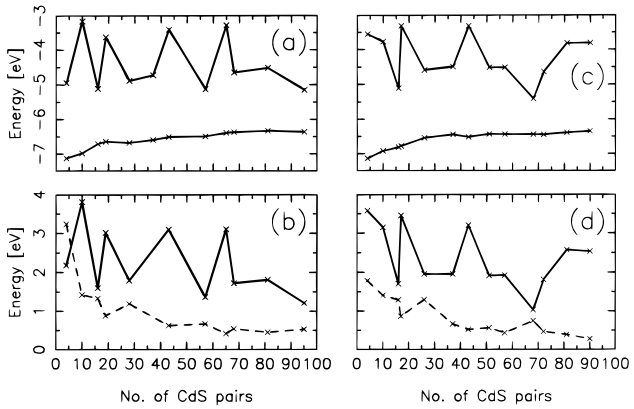

Figure 5. (a), (c): HOMO (lower curve) and LUMO (upper curve) energies; (b), (d): HOMO-LUMO gap (solid) compared with the total energy per CdS pair (dashed) for zinc blende (left column) and wurtzite (right column) with respect to the number of CdS pairs. The latter has been shifted by an additive constant.

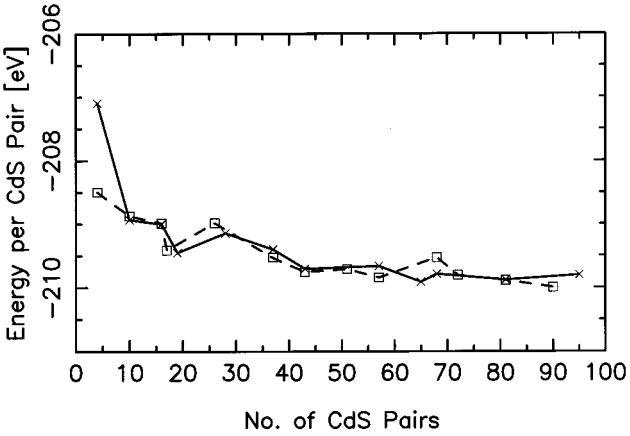

Figure 6. Variation in total energy per CdS pair as a function of cluster size for zinc blende- (solid curve) and wurtzite-derived clusters (dashed curve). The largest clusters have diameters of approximately 20 Å.

on variations of the cluster surface. Moreover, the surface localization of the LUMO has the consequence that HOMO and LUMO are spatially differently distributed within the cluster, which is important for low-energy transitions. This difference is in agreement with the recent experimental results of Lifshitz et al. for a similar system, cadmium selenide.[45,46] Although they studied exciton relaxation processes, one may to a first approximation assume that the relevant orbitals are very similar to the HOMO and LUMO and, accordingly, that our results can be used in analyzing these relaxation processes. Lifshitz et al. argued that the recombination took place at a low-symmetry site, e.g., one near the surface, and that the hole was delocalized to the whole cluster whereas the electron was localized to the surface. This result is accordingly supported by our findings.

On the other hand, theoretical studies of the surfaces of CdS and CdSe crystals have found[36,38] surface states just above the valence bands in contrast to our results here. In their study of CdSe clusters, Hill and Whaley[13] found, in some cases, surface states similar to ours. Also Ren and Ren[18] for CdS clusters and Pokrant and Whaley[27] for CdSe clusters found surface states appearing close to the bottom of the conduction states.

The sensitivity of the LUMO to surface variations can be seen clearly in Figure 5, which shows the HOMO and LUMO energies with increasing cluster size for zinc blende and wurtzite structures (upper panels). The results show a smooth dependence of the energy of the HOMO and an irregular, oscillating dependence of the energy of the LUMO on cluster size, which is a clear result of the HOMO being delocalized over the complete cluster and the LUMO being a surface state for all cluster sizes studied here. The lower part of the figure shows the HOMO-LUMO energy gap (solid curve) and the total energy per CdS pair (dashed curve). Here, it is seen that the more stable clusters have a larger energy gap. A correlation between energy gaps and stability is most often found for clusters of metal atoms (see, e.g., refs 47, 48), where the existence of magic numbers (i.e., of particularly stable clusters) is associated with the existence of a gap between occupied and unoccupied orbitals. Here, however, all clusters have a gap between HOMO and LUMO, and the here observed correlation between gap size and stability has, to our knowledge, not been observed previously for any semiconductor cluster. It may be speculated that samples of synthesized nanoparticles contain particularly many with sizes corresponding to the magic numbers and, accordingly, that the average energy gap between HOMO and LUMO is larger than what a more regular size distribution would suggest.

Finally, in Figure 6 we show the variation in the total energy per atom pair as a function of cluster size for the two different types of clusters. First of all, it is seen that these curves show an overall trend of an increasing binding energy when the cluster size increases. This can be taken as a direct consequence of the reduction in the ratio of surface atoms to bulk atoms. But, furthermore, the results show that the relative stability of wurtzite- and zinc blende-derived clusters varies as a function of cluster size. Since the total-energy differences are well beyond the inaccuracies found in Table 1, this finding is real and is actually in agreement with the observation of Weller and Eychmüller[46] who reported that CdS clusters of different sizes have different crystal structures (i.e., zinc blende or wurtzite structure). Since Weller and Eychmüller were not able to specify the precise number of atoms in their clusters, a direct comparison with our results is not possible.

4. Conclusions

In the present work we have applied a simplified LCAO-DFT-LDA scheme to study the structural and electronic properties of finite stoichiometric Cd_nS_n clusters. This work represents the first systematic study of the structural properties of larger semiconductor clusters.

The input for the method is obtained from first-principles calculations on diatomic molecules. To analyze the accuracy of the method for studies of larger systems, we first performed calculations on infinite, periodic crystals. These calculations were found to reproduce the experimentally found energetical *quasi*-degeneracy of the zinc blende and the wurtzite structures, but the zinc blende lattice was found to be the more stable structure. This is in contrast to the experiment. The obtained lattice parameters were in good agreement with those of other theoretical and experimental works.

By analyzing the radial distribution of the atoms for the finite clusters we could identify a surface region of roughly 2.5 Å thickness essentially independent of the size of the cluster. The Mulliken populations showed in addition that within this surface region the interatomic bonds have a larger ionic character than in the interior of the clusters where they are largely covalent. The structural data revealed also that the structural relaxations led to cadmium atoms moving toward the center of the cluster, whereas sulfur atoms move outward. This is important to know when attempting to passivate dangling bonds at the surfaces with surfactants, since they will then be bonded first of all to sulfur atoms. Furthermore, for the unpassivated clusters, the

sulfur atoms will most likely be the reaction partners in chemical reactions (e.g., in catalysis).

The HOMO was for all clusters delocalized over the entire cluster, whereas the LUMO was strongly localized to few atoms in the surface region. Thus, exciton relaxation processes depend strongly on surface effects, as also observed experimentally.

The results revealed also a close connection between stability and size of the band gap, which otherwise mainly is discussed for metal clusters. Finally, whereas the wurtzite structure is the more stable one (compared with zinc blende) for the infinite system, the relative stability of these two structures for the finite systems depends on their size.

Acknowledgment. One of the authors (M.S.) is grateful to Fonds der Chemischen Industrie for very generous support. Furthermore, this work was supported by the SFB 513 at the University of Konstanz.

References and Notes

(1) Henglein, A. In *Topics in Current Chemistry*, Vol. 143; Springer: Berlin, 1988.
(2) Yoffe, A. D. *Adv. Phys.* **1993**, *42*, 173.
(3) Nirmal, M.; Norris, D. J.; Kuno, M.; Bawendi, M. G.; Efros, A. L.; Rosen, M. *Phys. Rev. Lett.* **1995**, *75*, 3728.
(4) Alivisatos, A. P. *J. Phys. Chem.* **1996**, *100*, 13226.
(5) Gorer, S.; Hodes, G. In *Semiconductor Nanoclusters*; Kamat, P. V., Meisel, D., Eds.; Elsevier Science B.V.: Amsterdam, 1996.
(6) Yeh, C. Y.; Lu, Z. W.; Froyen, S.; Zunger, A. *Phys. Rev. B* **1992**, *45*, 12130.
(7) Federov, V. A.; Ganshin, V. A.; Korkishko, Yu. N. *Mater. Res. Bull.* **1993**, *28*, 59.
(8) Brus, L. E. *J. Chem. Phys.* **1983**, *79*, 5566.
(9) Brus, L. E. *J. Chem. Phys.* **1984**, *80*, 4403.
(10) Schmidt, H. M.; Weller, H. *Chem. Phys. Lett.* **1986**, *129*, 615.
(11) Ekimov, A. I.; Efros, A. L.; Ivanov, M. G.; Onushchenko, A. A.; Shumilov, S. K. *Solid State Commun.* **1989**, *69*, 565.
(12) Einevoll, G. T. *Phys. Rev. B* **1992**, *45*, 3410.
(13) Hill, N. A.; Whaley, K. B. *J. Chem. Phys.* **1994**, *100*, 2831.
(14) Lippens, P. E.; Lannoo, M. *Phys. Rev. B* **1989**, *39*, 10935.
(15) Rama Krishna, M. V.; Friesner, R. A. *J. Chem. Phys.* **1991**, *95*, 8309.
(16) Tomasulo, A.; Ramakrishna, M. V. *J. Chem. Phys.* **1996**, *105*, 3612.
(17) Mizel, A.; Cohen, M. L. *Phys. Rev. B* **1997**, *56*, 6737.
(18) Ren, S.-Y.; Ren, S.-F. *J. Phys. Chem. Solids* **1998**, *59*, 1327.
(19) Rabani, E.; Hetényi, B.; Berne, B. J.; Brus, L. E. *J. Chem. Phys.* **1999**, *110*, 5355.
(20) Pérez-Conde, J.; Bhattacharjee, A. K. *Solid State Commun.* **1999**, *110*, 259.
(21) Franceschetti, A.; Fu, H.; Wang, L. W.; Zunger, A. *Phys. Rev. B* **1999**, *60*, 1819.
(22) Eichkorn, K.; Ahlrichs, R. *Chem. Phys. Lett.* **1998**, *288*, 235.
(23) Wang, L.-W.; Zunger, A. *J. Phys. Chem. B* **1998**, *102*, 6449.
(24) Leung, K.; Pokrant, S.; Whaley, K. B. *Phys. Rev. B* **1998**, *57*, 12291.
(25) Wang, L.-W.; Zunger, A. *Phys. Rev. B* **1996**, *53*, 9579.
(26) Leung, K.; Whaley, K. B. *J. Chem. Phys.* **1999**, *110*, 11012.
(27) Pokrant, S.; Whaley, K. B. *Eur. Phys. J. D* **1999**, *6*, 255.
(28) Blaudeck, P.; Frauenheim, Th.; Porezag, D.; Seifert, G.; Fromm, E. *J. Phys. Cond. Matter* **1992**, *4*, 6389.
(29) Seifert, G.; Schmidt, R. *New J. Chem.* **1992**, *16*, 1145.
(30) Porezag, D.; Frauenheim, Th.; Köhler, Th.; Seifert, G.; Kaschner, R. *Phys. Rev. B* **1995**, *51*, 12947.
(31) Seifert, G.; Porezag, D.; Frauenheim, Th. *Int. J. Quantum Chem.* **1996**, *58*, 185.
(32) Hohenberg, P.; Kohn, W. *Phys. Rev.* **1964**, *136*, B864.
(33) Kohn, W.; Sham, L. J. *Phys. Rev.* **1965**, *140*, A1133.
(34) Landolt, Börnstein, *Numerical Data and Functional Relationships in Science and Technology, Group III: Crystal and Solid*; Madelung, O., Schulz, M., Eds.; 1982, Vol. 17b; and 1986, Vol. 22a. Springer-Verlag: Berlin, Heidelberg, New York, London, Paris, Tokyo.
(35) Yeh, C. Y.; Lu, Z. W.; Froyen, S.; Zunger, A. *Phys. Rev. B* **1992**, *46*, 10086.
(36) Wang, Y. R.; Duke, C. B. *Phys. Rev. B* **1988**, *37*, 6417.
(37) Horsky, T. N.; Brandes, G. R.; Canter, K. F.; Duke, C. B.; Paton, A.; Lessor, D. L.; Kahn, A.; Horng, S. F.; Stevens, K.; Stiles, K.; Mills, A. P., Jr. *Phys. Rev. B* **1992**, *46*, 7011.
(38) Schröer, P.; Krüger, P.; Pollmann, J. *Phys. Rev. B* **1994**, *49*, 17092.
(39) Bawendi, M. G.; Steigerwald, M. L.; Brus, L. E. *Annu. Rev. Phys. Chem.* **1990**, *41*, 477.
(40) Hill, N. A.; Whaley, K. B. *J. Chem. Phys.* **1993**, *99*, 3707.
(41) Gurin, V. S. *J. Phys. Chem.* **1996**, *100*, 869.
(42) Kobayashi, A.; Sankey, O. F.; Volz, S. M.; Dow, J. D. *Phys. Rev. B* **1983**, *28*, 935.
(43) Chang, K. J.; Froyen, S.; Cohen, M. L. *Phys. Rev. B* **1983**, *28*, 4736.
(44) Vogel, D.; Krüger, P.; Pollmann, J. *Phys. Rev. B* **1995**, *52*, R14316.
(45) Lifshitz, E.; Dag, I.; Litvin, I.; Hodes, G.; Gorer, S.; Reisfeld, R.; Zelner, M.; Minti, H. *Chem. Phys. Lett.* **1998**, *288*, 188.
(46) Lifshitz, E.; Dag, I.; Litvin, I.; Hodes, G. *J. Phys. Chem.* **1998**, *102*, 9245.
(47) de Heer, W. A. *Rev. Mod. Phys.* **1993**, *65*, 611.
(48) Brack, M. *Rev. Mod. Phys.* **1993**, *65*, 677.
(49) Weller, H.; Eychmüller, A. In *Semiconductor Nanoclusters*; Kamat, P. V., Meisel, D., Eds.; Elsevier Science B.V.: Amsterdam, 1996.